

Experimental observation of transient velocity-selective coherent population trapping in one dimension

Frank Vewinger* and Frank Zimmer†

Fachbereich Physik

Technische Universität Kaiserslautern

D-67663 Kaiserslautern

(Dated: December 11, 2018)

We report the observation of transient velocity-selective coherent population trapping (VSCPT) in a beam of metastable neon atoms. The atomic momentum distribution resulting from the interaction with counterpropagating σ_+ and σ_- radiation which couples a $J_g = 2 \leftrightarrow J_e = 1$ transition is measured via the transversal beam profile. This transition exhibits a stable VSCPT dark state formed by the two $|J = 2, m = \pm 1\rangle$ states, and a metastable dark state containing the $|J = 2, m = \pm 2\rangle$ and $|J = 2, m = 0\rangle$ states. The dynamics of the formation and decay of stable and metastable dark states is studied experimentally and numerically and the finite lifetime of the metastable dark state is experimentally observed. We compare the measured distribution with a numerical solution of the master equation.

PACS numbers: 32.80.Pj, 42.50.Vk, 33.80.Ps

Velocity-selective coherent population trapping (VSCPT) occurs by optical pumping of atoms into states with well defined momenta, which are decoupled from the light field. In a $J_g = 1 \leftrightarrow J_e = 1$ transition a dark state exists, which is a trapping state for zero momentum, leading to efficient cooling below the one-photon recoil limit [1, 2], which may be assisted by polarization-gradient precooling [3]. For ground state angular momenta $J_g > 1$ several dark states may exist. These are not necessarily eigenstates of the kinetic energy Hamiltonian and thus they are transient [4], not leading to population trapping. The stability of those states may be recovered by introducing m -dependent shifts of the Zeeman sublevels by a dc stark field [5] or additional laser fields [6]. The extension of VSCPT on three dimensions has also been discussed [7]. The existence of transient dark states has for instance been used to demonstrate a multiple beam atomic interferometer in cesium [8]. Furthermore, for specific polarizations of the laser fields the existence of high-velocity dark states has been shown [9]. Recently studies of velocity-selective coherent population trapping and its relation to electromagnetically induced transparency (EIT) and atomic entanglement were reported [10].

For a $J_g = 2 \leftrightarrow J_e = 1$ transition coupled by counter-propagating σ_+ and σ_- beams the existence of transient VSCPT has been shown theoretically [4], but to the best of our knowledge experimental momentum distributions have not been reported. In particular the metastability of some of the dark states has not been directly shown in the experiment. We present measurements that clearly show the signature of a stable and a transient dark state in the momentum distribution of a beam of neon atoms

in the metastable state 3P_2 .

The coupling scheme for the $J_g = 2 \leftrightarrow J_e = 1$ transition driven by σ_+ and σ_- irradiation with equal frequency is shown in Figure 1. The system is characterized by the Hamiltonian,

$$H = \frac{\mathbf{p}^2}{2M} + \hbar\omega_0 P_e + V_{AL}, \quad (1)$$

where P_e is the projector onto the excited states, \mathbf{p} the momentum operator and M is the atomic mass. The interaction Hamiltonian $V_{AL} = V_\Lambda + V_{IW}$ consists of two parts. One describes the Λ -system $\{g_{-1}, e_0, g_{+1}\}$, the other the inverted-W configuration $\{g_{-2}, e_{-1}, g_0, e_{+1}, g_{+2}\}$. In the rotating wave approximation the two terms read

$$V_\Lambda = \sum_q \frac{\hbar}{2} \sqrt{\frac{3}{10}} \{ \Omega_+ |e_0, q\rangle \langle g_{-1}, q - \hbar k| + \Omega_- |e_0, q\rangle \langle g_{+1}, q + \hbar k| \} \exp(-i\omega_L t) + h.c., \quad (2)$$

$$V_{IW} = \sum_q \frac{\hbar}{2} \left[\sqrt{\frac{6}{10}} \Omega_+ |e_{-1}, q - \hbar k\rangle \langle g_{-2}, q - 2\hbar k| + \sqrt{\frac{1}{10}} [\Omega_- |e_{-1}, q - \hbar k\rangle + \Omega_+ |e_{+1}, q + \hbar k\rangle] \langle g_0, q| + \sqrt{\frac{6}{10}} \Omega_- |e_{+1}, q + \hbar k\rangle \langle g_{+2}, q + 2\hbar k| \right] e^{-i\omega_L t} + h.c., \quad (3)$$

where Ω_+ (Ω_-) is the Rabi frequency of the coupling laser for the transition $|g_0\rangle \leftrightarrow |e_{+1}\rangle$ ($|g_0\rangle \leftrightarrow |e_{-1}\rangle$).

The interaction Hamiltonian V_{AL} separates the atomic states into two sets of momentum families, which are coupled to each other only by spontaneous emission. These are

$$\mathfrak{F}^\Lambda(q) = \{ |e_0, q\rangle, |g_{-1}, q - \hbar k\rangle, |g_{+1}, q + \hbar k\rangle \} \quad (4)$$

$$\mathfrak{F}^{IW}(q) = \{ |g_{-2}, q - 2\hbar k\rangle, |e_{-1}, q - \hbar k\rangle, |g_0, q\rangle, |e_{+1}, q + \hbar k\rangle, |g_{+2}, q + 2\hbar k\rangle \}. \quad (5)$$

*Electronic address: vewinger@physik.uni-kl.de

†Electronic address: zimmer@physik.uni-kl.de

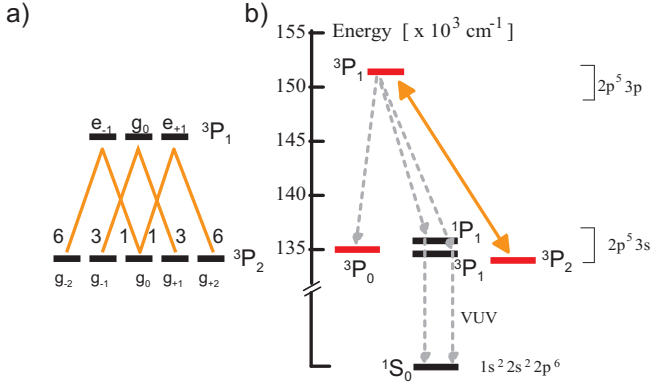


FIG. 1: a) Coupling scheme for the $J = 2 \leftrightarrow J = 1$ transition driven by σ_+ and σ_- polarized light. The numbers are the squares of the ratios of the Clebsch-Gordan coefficients. b) Level scheme of neon including the relevant levels for the experiment.

The $\mathfrak{F}^\Lambda(q)$ family involves two states which have for $q = 0$ the same energy. Thus two-photon resonance within the Λ -system can be maintained using a single laser frequency and the dark state $|\Psi_{NC}^\Lambda(q=0)\rangle$ formed by the members of this family will be stable. The $\mathfrak{F}^{IW}(q)$ family involves states with different momenta. Thus two-photon resonance between the states $|g_{\pm 2}\rangle$ and $|g_0\rangle$ can not be maintained with a single laser frequency. Furthermore the dark state $|\Psi_{NC}^{IW}\rangle$ formed within this family is no eigenstate of the kinetic energy Hamiltonian $\mathbf{p}^2/2M$. The lifetime τ_{IW} of this state has been calculated perturbatively, assuming that all Clebsch-Gordan coefficients are equal [4]. The two dark states read

$$|\Psi_{NC}^\Lambda\rangle = \frac{1}{\sqrt{\Omega_+^2 + \Omega_-^2}} \times [\Omega_- |g_{-1}, q - \hbar k\rangle - \Omega_+ |g_{+1}, q + \hbar k\rangle], \quad (6)$$

$$|\Psi_{NC}^{IW}\rangle = \frac{1}{\sqrt{\Omega_+^4 + 6\Omega_+^2\Omega_-^2 + \Omega_-^4}} \left[\Omega_-^2 |g_{-2}, q - 2\hbar k\rangle - \sqrt{6}\Omega_+\Omega_- |g_0, q\rangle + \Omega_+^2 |g_{+2}, q + 2\hbar k\rangle \right]. \quad (7)$$

For interaction times $\tau < \tau_{IW}$ both dark states appear as trapping states for $q = 0$, giving rise to a momentum distribution with peaks at $-2\hbar k, -\hbar k, 0, \hbar k$ and $2\hbar k$. For interaction times $\tau > \tau_{IW}$ the contribution of $|\Psi_{NC}^{IW}\rangle$ vanishes and only two peaks at $\pm\hbar k$ remain in the momentum distribution.

In the experiment, a beam of neon atoms emerges from a liquid nitrogen cooled discharge nozzle source. A fraction of the order of 10^{-4} of the atoms is in the metastable states 3P_0 or 3P_2 of the $2p^5 3s$ electronic configuration [11]. The flow velocity of the atoms is about 470 ms^{-1} with a width of the velocity distribution of about 100 ms^{-1} (FWHM). The beam is collimated by a $50 \mu\text{m}$ and a $10 \mu\text{m}$ slit positioned 144 cm apart, corresponding to a width of the transversal velocity distribu-

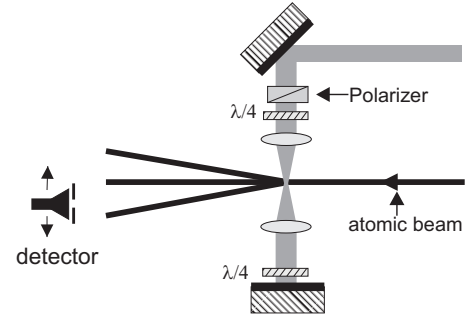


FIG. 2: Schematic setup of the experiment. The cylindrical lenses have a focal length of 250 mm and they are in a confocal arrangement. Further details can be found in the text.

tion of about $0.15\hbar k$. The population of the metastable 3P_0 state is depleted by optical pumping before the atoms interact with the circular polarized laser beams in a region 20 cm downstream of the second slit. The spatial distribution of the atoms in the states 3P_0 and 3P_2 is measured 120 cm downstream of the interaction zone using a movable channeltron detector behind an entrance slit of $25 \mu\text{m}$ width, leading to a resolution of the transverse momentum of $\Delta p \approx 0.2\hbar k$. In the interaction region the magnetic field is actively compensated to less than $1 \mu\text{T}$, to assure the degeneracy of all Zeeman states to within better than 130 kHz. The laser beam passes through a polarizer, two quarter wave plates and optionally two cylindrical lenses before being retroreflected (Fig. 2), establishing a counterpropagating $\sigma_+ - \sigma_-$ -configuration. In order to realize different interaction times three different setups for the width of the laser beams were used. The first setup uses cylindrical lenses in a confocal arrangement with the atomic beam crossing the laser beam near the focus. The transit time of the atoms through the laser beam is estimated to be a few 100 ns, corresponding to $\Gamma t \approx 10$, where Γ is the width of the transition between the 3P_1 and 3P_2 state. The laser beam profile at the position of the atomic beam is not measured directly but inferred from the dimensions of the optical setup. The laser beams are parallel to within 10^{-5} rad. The peak Rabi frequency is in the order of 500 MHz and the lasers are tuned from the $|g_0\rangle \leftrightarrow |e_0\rangle$ resonance by 100 MHz to reduce the influence of stray light from the windows. To increase the interaction between the atoms and the light field the cylindrical lenses can be removed, leading to an interaction time of $\Gamma t = 200$. Using a telescope in front of the polarizer the beam diameter can be increased to 8 mm, leading to an interaction time of $\Gamma t = 800$.

Figure 3 shows the initial momentum distribution (grey area) and the result for a short interaction time of $\Gamma t \approx 10$ (squares). Five peaks at $\pm 2\hbar k, \pm\hbar k$ and zero momentum are clearly resolved. The asymmetry of the momentum distribution is due to different intensities of the σ_+ and σ_- beams: The retroreflected beam passes twice through a window and the (uncoated) cylindrical lens before crossing the atomic beam, resulting in a lower

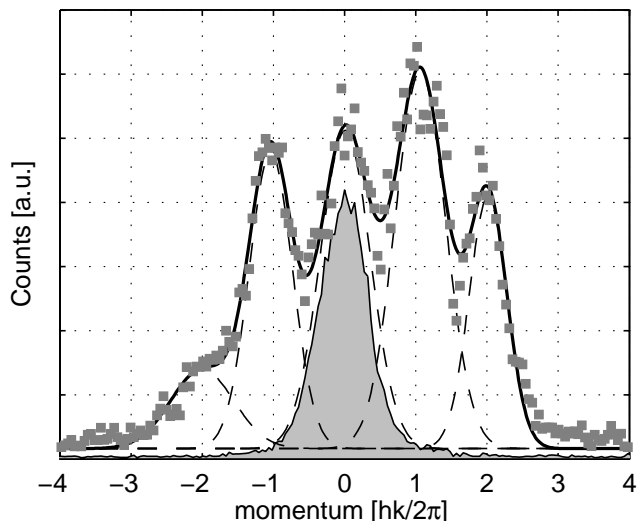


FIG. 3: Transverse atomic momentum profile after a short interaction ($\Gamma t < 10$). The grey area shows the initial momentum distribution (scaled down), the dashed lines are gaussian fits to the individual peaks. The full line is the sum of the gaussian fits.

intensity in the retroreflected beam. Thus the Rabi frequencies of the two laser beams are not equal, $\Omega_+ \neq \Omega_-$, therefore we find an asymmetric population distribution within the dark states (6) and (7). This is also confirmed by numerical simulations of the process. The peak at zero momentum also contains contributions from population in the 3P_0 state, which is populated by spontaneous emission from the upper state 3P_1 during the interaction.

In order to do a supplementary test that we observe velocity-selective coherent population trapping the retroreflected beam was slightly tilted. A sufficient overlap of both beams was sustained but the retroreflected beam interacts with the atoms after the dark states have been populated. Due to optical pumping the population of the states $|g_{-2}\rangle$, $|g_{-1}\rangle$ and $|g_0\rangle$ is depleted, and the height of the peaks at negative momenta decrease, since the internal and external states in the dark states are strongly correlated. The measurement with tilted lasers is shown in figure 4, which shows good agreement of experimental and calculated profiles.

When increasing the laser beam diameter with a telescope to 8 mm the interaction time is of the order $\Gamma t \approx 800$. We then observe the transversal beam profile shown in figure 5. The peaks at $\pm 2\hbar k$ are no longer seen and only the stable dark state $|\Psi_{NC}^\Lambda\rangle$ survives, reflected by the peaks at the momenta $\pm \hbar k$. The peak at zero momentum appears because the state 3P_0 is populated by spontaneous emission during the process of dark state preparation.

We compare the measured data to a solution of the generalized optical Bloch equations in the family momentum basis [2], neglecting spontaneous decay to other

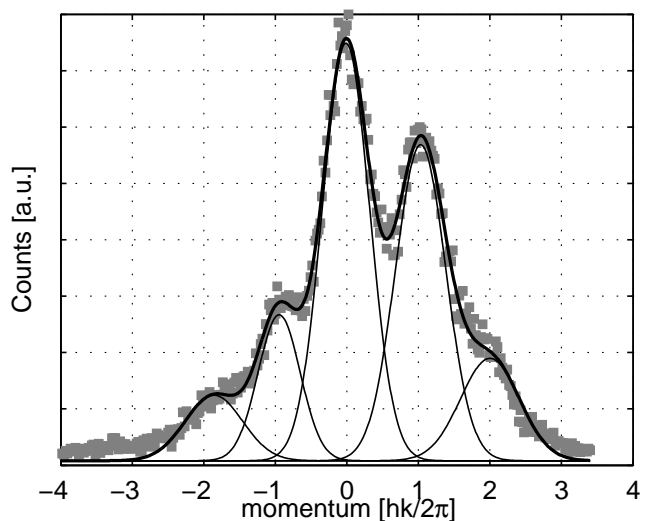


FIG. 4: Transversal momentum distribution after the interaction with a tilted retroreflected laser. The dashed lines are gaussian fits to the individual peaks, the solid line is their sum. The depopulation of the peaks with negative momentum is clearly visible.

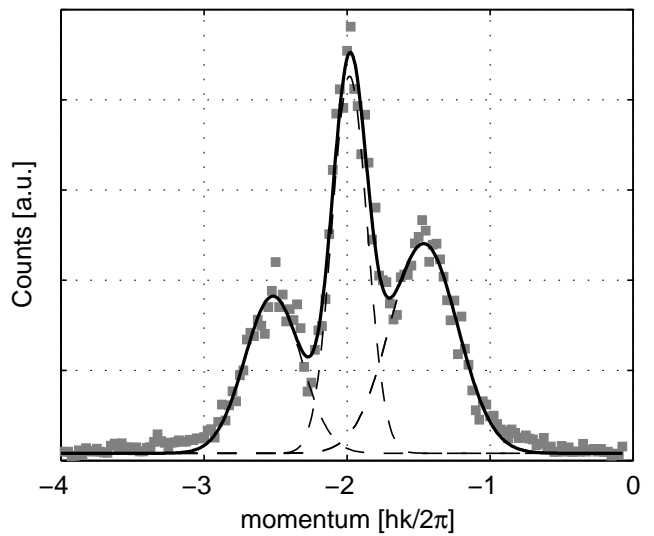


FIG. 5: Transverse atomic momentum profile after an interaction of $8 \mu s$ ($\Gamma t \approx 800$). The lines are gaussian fits to the peaks. The peaks at $p = \pm \hbar k$ reflect the stable dark-state $|\Psi_{NC}^\Lambda(q=0)\rangle$.

levels outside the system. The Bloch equation reads

$$\begin{aligned} \dot{\rho} = & -\frac{i}{\hbar} [H, \rho] \\ & - \frac{\Gamma}{2} [(\Delta^+ \cdot \Delta^-) \rho + \rho (\Delta^- \cdot \Delta^+)] \\ & + \frac{3\Gamma}{8\pi} \int d^2\Omega \sum_{\epsilon \perp \mathbf{n}} (\Delta^+ \cdot \epsilon)^\dagger \exp(-i\mathbf{k}\mathbf{n} \cdot \mathbf{R}) \rho \\ & \times \exp(i\mathbf{k}\mathbf{n} \cdot \mathbf{R}) (\Delta^+ \cdot \epsilon), \end{aligned} \quad (8)$$

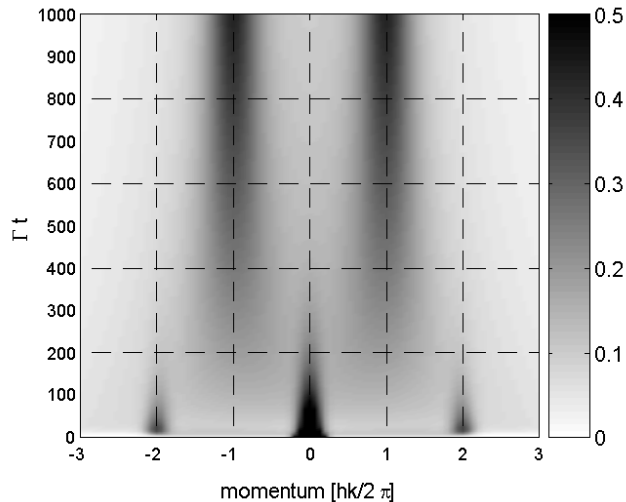


FIG. 6: Dynamics of the momentum distribution, derived from a numerical solution of the Bloch equations (8). The population is encoded by the greyscale given on the right.

where Δ_{\pm} are the lowering and raising parts of the reduced dipole operator and ϵ is the polarization vector [12]. \mathbf{R} is the position operator of the center of mass which acts only on the external variables. The second term describes the decrease of the excited-state populations and coherences resulting from spontaneous emission; the term under the integral over all solid angles (third term) describes the feeding of the ground-state population and coherences by spontaneous emission of a fluorescence photon into the solid angle around the direction \mathbf{n} , with energy $\hbar c k$ and polarization $\epsilon \perp \mathbf{n}$. The explicit form of the differential equations for the density matrix elements are given in [13]. The equations were integrated stepwise with a resolution of $1/50\Gamma^{-1}$ in time and $\hbar k/20$ in momentum space on an interval of $[-8\hbar k, 8\hbar k]$. The calculations were done for a Rabi frequency of 0.3Γ with no time dependence. The initial momentum distribution is given by a gaussian profile of width $\Delta q = 0.15\hbar k$ centered at $p = 0$, which is taken from the experiment. Initially all Zeeman states in the 3P_2 manifold are equally populated. The results are shown in Fig. 6.

For a short interaction time of $\Gamma t < 15$, the atoms absorb a photon from one of the laser beams, followed by stimulated emission into the other beam. This leads to a change in momentum by $\Delta p = \pm 2\hbar k$, and peaks in the momentum distribution at $p = \pm 2\hbar k$ appear. This

process of stimulated raman transitions causes an efficient population transfer to the dark state $|\Psi_{\text{NC}}^{IW}(q=0)\rangle$, characterized by a momentum distribution located at $p = \pm 2\hbar k$ and $p = 0$. Absorption of a photon followed by spontaneous emission results in a random walk in momentum space due to the emission of photons in an arbitrary direction. This diffusive process successively populates the stable dark state $|\Psi_{\text{NC}}^{\Lambda}(q=0)\rangle$ which is characterized by the two peaks at momentum $p = \pm \hbar k$ in the momentum representation. Due to the statistical nature of this process the population of the dark state $|\Psi_{\text{NC}}^{\Lambda}(q=0)\rangle$ increases for longer interaction times, $\Gamma t > 200$.

The calculations show good agreement with the measured data. The calculations show a structure with five peaks at $-2\hbar k, \dots, 2\hbar k$ for $\Gamma t \approx 100 - 200$, while the measurements yield this structure for $\Gamma t \approx 10 - 20$. The values for the interaction time are not directly comparable, as the calculations were done for a constant Rabi frequency, while in the experiment the light fields have a gaussian shape. Furthermore the widths of the measured peaks is smaller than expected from the simulations, which is due to neglecting spontaneous emission out of the system $\{{}^3P_1, {}^3P_2\}$.

The measurements for a long interaction time of $\Gamma t = 800$ (Fig. 5) show good agreement with the numerical results. The population of the stable dark state (6) is rising, while the population of other states is decaying into this dark state via the diffusion in momentum space due to the spontaneous emission of photons.

In this work we have presented measurements which directly demonstrate the existence of transient dark states with a well defined momentum distribution in a m -state manifold of a $J_g = 2$ -level coupled to a level with $J_e = 1$ by counterpropagating σ_+ and σ_- radiation. The measured data show good agreement with quantum density matrix calculations for the velocity distribution for short as well as longer interaction times. For a quantitative analysis more detailed experiments as well as calculations including spontaneous emission into other states than the 3P_2 -state are needed.

We thank K. Bergmann and M. Fleischhauer for their support, discussions and helpful comments on the manuscript. We thank M. Heinz for his contribution to the experiments. This work was supported by the Deutsche Forschungsgemeinschaft (Project Be 623/32) and under the Graduiertenkolleg 792 'Nichtlineare Optik und Ultrakurzzeitphysik'.

-
- [1] A. Aspect, E. Arimondo, R. Kaiser, N. Vansteenkiste, and C. Cohen-Tannoudji, *Physical Review Letters* **61**, 826 (1988).
 [2] A. Aspect, E. Arimondo, R. Kaiser, N. Vansteenkiste, and C. Cohen-Tannoudji, *Journal of the Optical Society of America B* **6**, 2112 (1989).

- [3] M. S. Shahriar, P. R. Hemmer, M. G. Prentiss, P. Marte, J. Mervis, D. P. Katz, N. P. Bigelow, and T. Cai, *Physical Review A* **48**, R4035 (1993).
 [4] F. Papoff, F. Mauri, and E. Arimondo, *Journal of the Optical Society of America B* **9**, 321 (1992).
 [5] M. A. Ol'shanii, **24**, L583 (1991).

- [6] C. Menotti, G. Morigi, J. Muller, and E. Arimondo, *Physical Review A (Atomic, Molecular, and Optical Physics)* **56**, 4327 (1997).
- [7] M. Ol'shanii and V. Minogin, *Optics Communications* **89**, 393 (1992).
- [8] M. Weitz, T. Heupel, and T. W. Hänsch, *Physical Review Letters* **77**, 2356 (1996).
- [9] M. Widmer, M. R. Doery, M. J. Bellanca, W. F. Buell, T. H. Bergeman, and H. J. Metcalf, *Physical Review A* **53**, 946 (1996).
- [10] M. Kiffner and K.-P. Marzlin (2005), [quant-ph/0501092](https://arxiv.org/abs/quant-ph/0501092).
- [11] J. M. Weber, K. Hansen, M.-W. Ruf, and H. Hotop, *Chem. Phys.* **239**, 271 (1998).
- [12] Y. Castin, H. Wallis, and J. Dalibard, *Journal of the Optical Society of America B* **6**, 2047 (1989).
- [13] H. Wallis, *Physics Reports* **255**, 203 (1995).